

Modelling the tidal currents using the lattice Boltzmann method with the lid-driven cavity problem

Andrew Cunningham, Jian Zhou and Jon Shiach

School of Computing, Mathematics and Digital Technology

Manchester Metropolitan University

United Kingdom

November 2019

Abstract: Keywords: Lattice Boltzmann method, single relaxation time, lid-driven cavity, Dover harbour

1 Introduction

Dover harbour, considered to be busiest passenger harbour in Britain, will experience increased traffic and delays with Brexit. With this harbour being a major hub for transport of both goods and services a deeper understanding of the fluid currents that may affect this harbour and the vessels it shelters is desired.

Shallow seas, such as those seen in the Strait of Dover, differ from their larger, deeper counterparts due to the geostrophic acceleration, coastal boundaries, etc. acting upon them (Bowden 1956). These factors influence the tidal currents greatly. Breakwaters have a considerable impact and prevent turbulent erratic flow from entering the harbour and preventing travel. The breakwater around Dover harbour started to be built within 1847 to decrease these influences (Vernon-Harcourt 1885). The water renovation and flushing from the harbour has been studied by Sanchez-Arcilla (2002) as has the effect of having two entrances to the harbour. This paper will take a brief look into the effect the breakwater at Dover harbour has upon the inner harbour itself.

The effect of both the North Sea and the English Channel give a residual circulation pattern that ebbs and flows high and low tides (Prandle et al. 1993). These tides directly affect the harbour by flowing across the top of it thus creating small inner vortices both inside and outside of the harbour. The vortices created by these two differing flows has been observed both in Dover and in Calais (Latteux 1980).

Using satellite imagery areas of the harbour were analysed and drawn to represent the more complicated geometry of the harbour. Then a constant horizontal initial force was applied to the top of the domain. This is to represent a constant flow of a tidal current from the English Channel.

For these simulations a reconstruction of the Dover harbour has been attempted using a lid-driven cavity problem to represent the effect of tidal currents from the English Channel across the harbour.

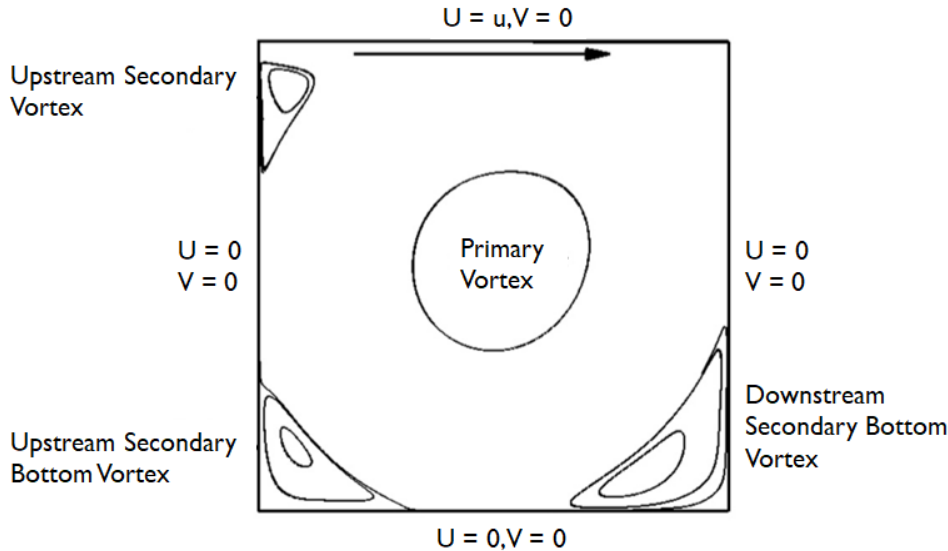


Figure 1: The lid-driven cavity problem as proposed by Perumal (2013)

The lid-driven cavity flow problem has been a useful benchmark case to evaluate numerical methods (U. Ghia, K. N. Ghia, and Shin 1982b) for solutions towards the incompressible Navier-Stokes equations. With a plethora of industrial and engineering applications, such as coating and printing, many find this problem an attractive case to study (Perumal and Dass 2013). The cavity creates distinct features such as the vortices shown in Figure 1 which change at differing Reynolds numbers Re . These results have been studied extensively which makes the lid-driven cavity an ideal candidate with which to test new computational numerical methods.

The lattice Boltzmann method has shown promise as a modern numerical method for solving incompressible flow problems (Guo, Shi, and Wang 2000) and is a successor to the lattice gas automata, (Wolf-Gladrow 2000) which comprised of Boolean logic to determine where particles lay within a system. The role of the lattice Boltzmann method is to describe the simulation through the mesoscopic range, the bridge between the microscopic and the macroscopic worlds (McNamara and Zanetti 1988). In this range a group of particles are considered rather than mapping the complete particle interactions. Then the macroscopic quantities are developed and associated to the system, necessary for the formulation of the Navier-Stokes equations. This allows the method to be easily paralleled with other machines (Huang et al. 2015).

Within this paper a idealised version of Dover harbour will be generated using the lid-driven cavity as a benchmark case using the lattice Boltzmann method. Then the model will be tested using varying levels of Reynolds numbers, Re , to examine the harbour within more turbulent waters.

2 Methodology

For these simulations a 2D single relaxation time approach was used. For this a lattice configuration of 9 vertices within a square lattice was used also known as a D2Q9 approach as seen in Figure 2. The single relaxation method, also known as the Bhatnagar, Gross, Krook method or LBGK for short (Bhatnagar, Gross, and Krook 1953) is defined by

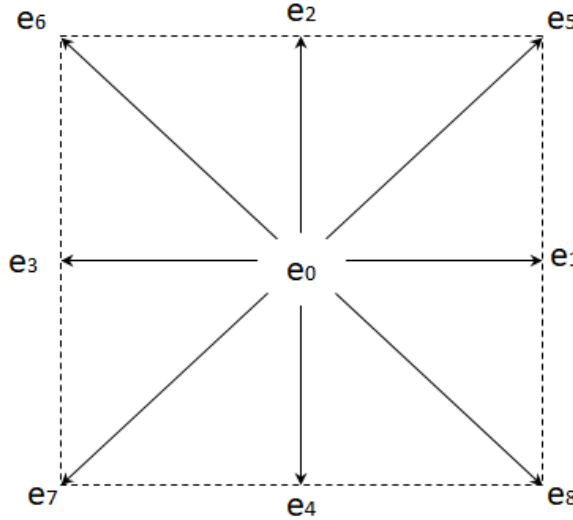


Figure 2: A two-dimensional 9 vertices lattice

$$f_i(x + e_i \delta x, t + \delta t) = f_i(x, t) - \frac{(f_i(x, t) - f_i^{eq}(x, t))}{\tau} \quad (1)$$

where $f_i(x, t)$ and $f_i^{eq}(x, t)$ are the particle and equilibrium distribution functions at (x, t) , e_i is the particle velocity along the i th direction and τ is the relaxation-time parameter that controls the rate of approach to the equilibrium which is related to the kinematic viscosity ν by

$$\tau = \frac{6\nu + 1}{2} \quad (2)$$

The kinematic viscosity is measured using lattice units. With a D2Q9 approach only nine velocity vectors are used such that the discrete velocity set $i = 1, \dots, 9$, where the discrete velocity set e_i is defined as

$$e_i = \begin{cases} 0, & i = 9 \\ c(\cos((i-1)\pi/4), \sin((i-1)\pi/4)), & i = 1, 2, 3, 4 \\ \sqrt{2}c(\cos((i-1)\pi/4), \sin((i-1)\pi/4)), & i = 5, 6, 7, 8 \end{cases}$$

where c is the lattice speed.

In the D2Q9 square lattice the equilibrium distribution function proposed is

$$\begin{aligned} f_i &= \rho w_i [1 - \frac{3}{2}u^2], & i &= 0, \\ f_i &= \rho w_i [1 + 3(e_i u) + \frac{9}{2}(e_i u)^2 \frac{3}{2}u^2], & i &= 1, 2, 3, 4, \\ f_i &= \rho w_i [1 + 3(e_i u) + \frac{9}{2}(e_i u)^2 \frac{3}{2}u^2], & i &= 5, 6, 7, 8, \end{aligned} \quad (3)$$

where u is the velocity and w_i is the lattice weights given by

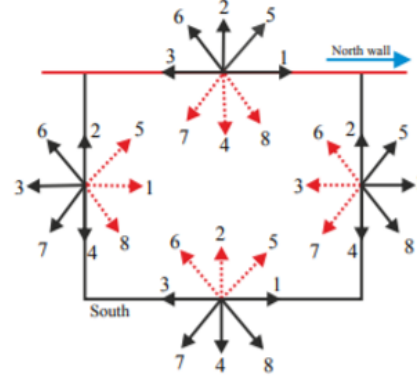


Figure 3: The lid-driven cavity problem boundary conditions (Mohammed and Reis 2017)

$$w_i = \begin{cases} \frac{4}{9}, & i = 9 \\ \frac{1}{9}, & i = 1, 2, 3, 4 \\ \frac{1}{36}, & i = 5, 6, 7, 8 \end{cases}$$

The macroscopic quantities, density ρ and momentum density ρu , are calculated using the distribution function f_i .

$$\rho = \sum_{i=1}^N f_i \quad (4)$$

$$\rho u = \sum_{i=1}^N f_i e_i \quad (5)$$

Where N is the maximum amount of discrete vertices, in this case 9. The density is determined from the particle distribution function where the density and velocities satisfy the Navier-Stokes equation (Perumal and Dass 2013). This can be shown using the Chapman-Enskog expansion (Nie and Martys 2007).

2.1 Boundary Conditions

For the current simulations a combination of both non-slip and Zou-He boundary conditions have been implemented. For the non-slip, also known as a traditional bounce-back boundary condition, the particle is reflected from a solid surface. These conditions have been used at the solid boundaries of the harbour and across the south, east and west boundaries of the cavity as seen in Figure 7. The LBM solves these conditions through

$$\begin{aligned} f_1 &= f_3, & f_2 &= f_4 \\ f_5 &= f_7, & f_6 &= f_8. \end{aligned} \quad (6)$$

For the north boundary Zou-He boundary conditions are applied (Zou and He 1997). As this is the inlet to the simulation particular care must be exercised for the length of the boundary including the corners. These conditions work by utilising the known vertices and parameters and extrapolating them for the unknown variables to form a complete set to avoid any undesired errors. Take the northern boundary as an example, currently only six vertices are known, e_1, e_2, e_3, e_5, e_6

and e_9 , therefore using these conditions the vertices flowing into the cavity can be fully expressed. The northern boundary condition is defined by

$$\begin{aligned}\rho_{in} &= \frac{1}{1+u_y}(f_9 + f_1 + f_3 + 2(f_2 + f_5 + f_6)) \\ f_4 &= f_2 - \frac{2}{3}\rho u_y \\ f_7 &= f_5 + \frac{1}{2}(f_2 + f_4) - \frac{1}{2}\rho u_x - \frac{1}{6}\rho u_y \\ f_8 &= f_6 + \frac{1}{2}(f_2 + f_4) + \frac{1}{2}\rho u_x - \frac{1}{6}\rho u_y\end{aligned}\tag{7}$$

where u_x and u_y are the horizontal and vertical velocity respectively and ρ_{in} is the density across the inlet.

A particular point that needs more consideration is the corners of the inlet. For these areas only four velocity vectors are known however approximations can be inferred through extrapolation using Zou-He's conditions. Using the top right corner of the simulation as an example, which will be defined as ne , the four known vertices are e_1, e_2, e_5 , and e_9 . Using a configuration expressed within (Mohammed and Reis 2017) the ne corner condition can be defined by

$$\begin{aligned}\rho_{ne} &= f_9 + 2f_1 + 4f_5 + 2f_2 \\ f_3 &= \frac{2\rho_{ne}}{3} - f_9 - f_1 \\ f_4 &= \frac{2\rho_{ne}}{3} - f_9 - f_2 \\ f_6 &= \frac{\rho_{ne}}{6} - f_2 - f_5 \\ f_8 &= \frac{\rho_{ne}}{6} - f_1 - f_5 \\ f_7 &= \frac{-2\rho_{ne}}{3} + f_9 + f_2 + f_3 + f_6\end{aligned}\tag{8}$$

where ρ_{ne} is the density at the ne corner.

3 Validation

The lid-driven cavity model shown in Figure. 1 has an initial horizontal velocity u_0 across the top of the cavity with each other boundary being a solid wall. This causes the flow to spiral and create distinct vortices within the cavity. The more distinct change occurs when increasing the Re of the cavity. The Re is related to the kinematic viscosity ν by

$$Re = \frac{u_0 L}{\nu}\tag{9}$$

where u_0 is the initial velocity and L is the characteristic length. This increase in the Re increases the turbulence of the flow which accentuates the distinct vortices features found within the cavity flow problem.

The model was validated against the results of Ghia (U. Ghia, K. N. Ghia, and Shin 1982a) at varying levels of Re . For this both the horizontal and vertical velocity were recorded at the centre of the simulation and compared with Ghia's results. A good level of accuracy was found when comparing the results.

An L2 error was also examined before starting the more complex simulations to test the convergence of the model.

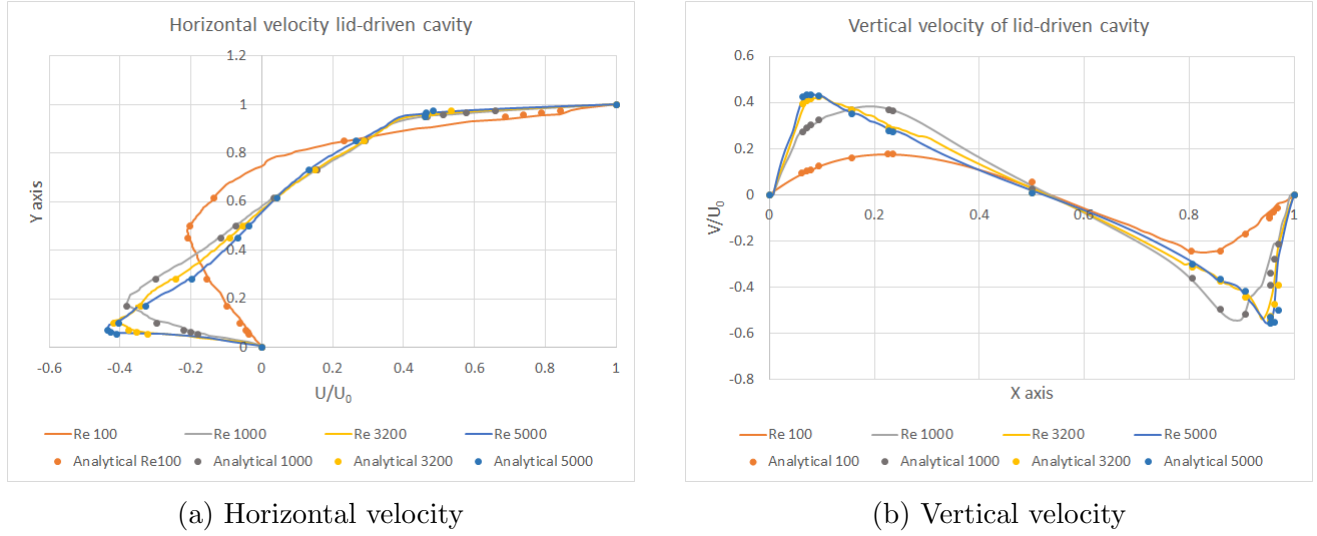


Figure 4: Velocity graphs compared with Ghia's results (1982)

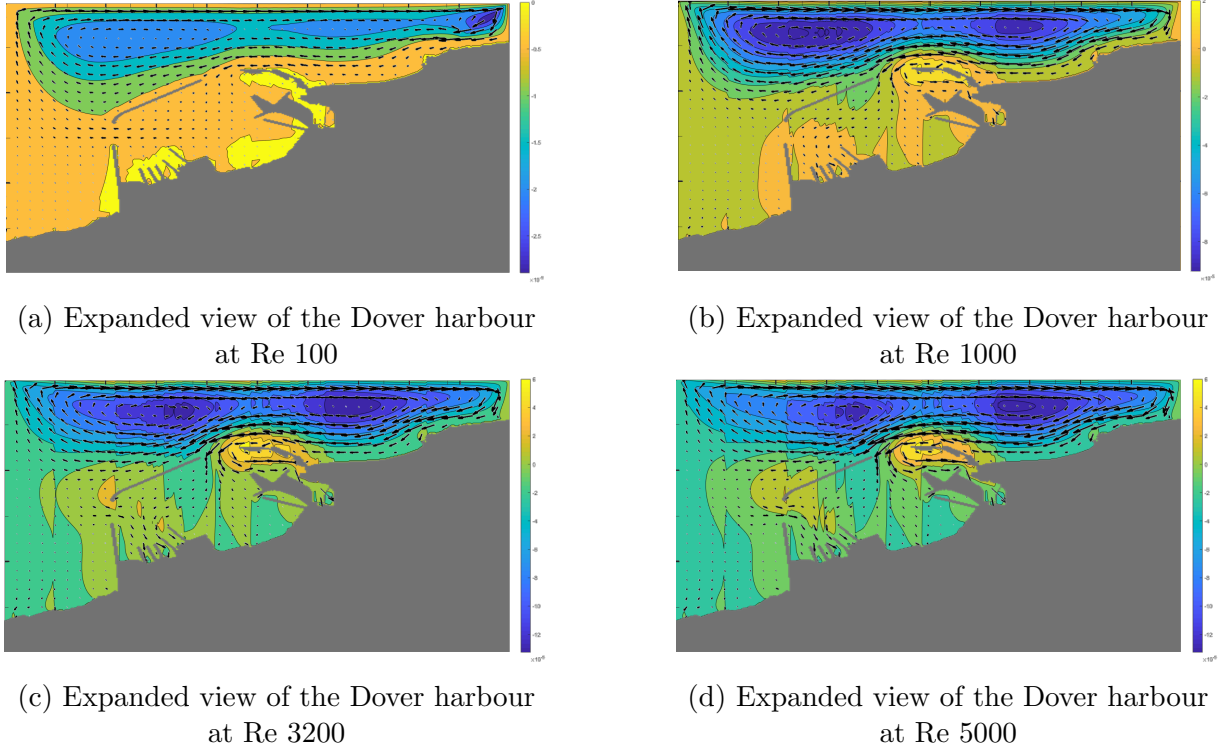


Figure 5: A zoomed out look of Dover Harbour and the surrounding geographical area using the lid-driven cavity problem

4 Results

Two cases have been generated for these simulations. The first being an expanded view of the harbour and the surrounding landscape and the second taking a closer look into the harbour itself.

Observing the flow being created by the lid-driven cavity problem within the lower Re there seem to be a more consistent flow within the harbour matching the speed of the lid. As shown

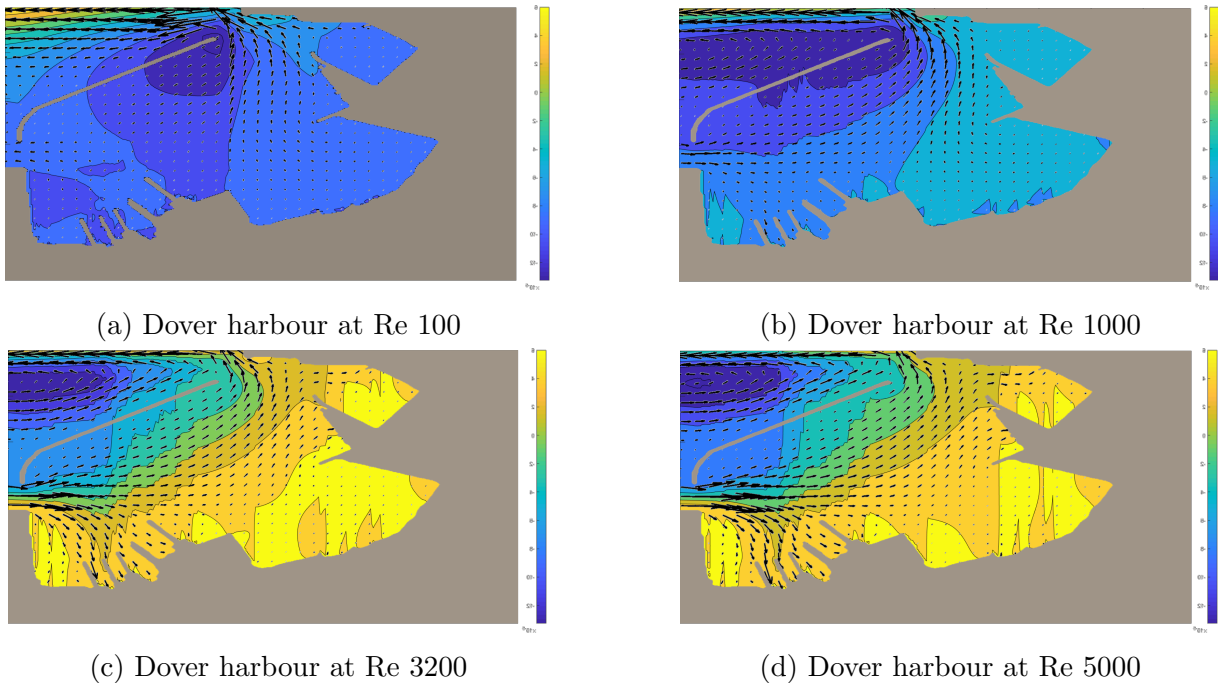


Figure 6: A zoomed in simulation of Dover Harbour where the inlet is closer to the breakwater

in Figures 5a and 5b most of the flow follows the same horizontal direction, therefore the flow generally stays positive. There are two distinctive elliptical vortices being created outside the harbour. The breakwater seems to stop the flow of these vortices inside the harbour allowing for a more consistent speed of the flow within the harbour.

At greater Re flows, shown in Figures 5c and 5d become much more turbulent as expected. The flow speeds within the harbour vary significantly more than the lower Re counterparts. The flow within the harbour looks to be flowing counter to the inlet. There seems to be two vortices being formed close to the solid boundaries of the breakwater and the rightmost inlet. Consistently the two vortices forming outside the breakwater do not change shape or form at all levels of Re tested.

The tidal current generated by the lid causes a fast jet stream to be flowing past the harbour area. However the greatest differences are examined at the top of the simulation with two distinctive vortices being created allowing for a change in velocity of about magnitude 3.

For the zoomed in simulations seen in Figures 6a to 6d a similar circumstance exists where the lower Re simulations have significantly less variation in regards to the velocity within the harbour. Within each simulation however a vortex was created outside the breakwater closest to the inflow. This vortex increased in size and variance of speed with each increase in Re .

Both Figures 6a and 6b seem to be laminar with very little interactions or changes within the harbour. However with Figures 6c and 6d small vortices are created within the harbour which could damage smaller vessels. The most significant change is on the southern entrance to the harbour where the larger ferries will dock. According to the model a powerful current coming in from the English Channel enters the harbour causing drastic changes in the flow velocity within. The velocity changes are of magnitude 2 which is significant.

The Mean Spring Tidal Currents report for Dover Harbour (Masters 2019) reports when and how

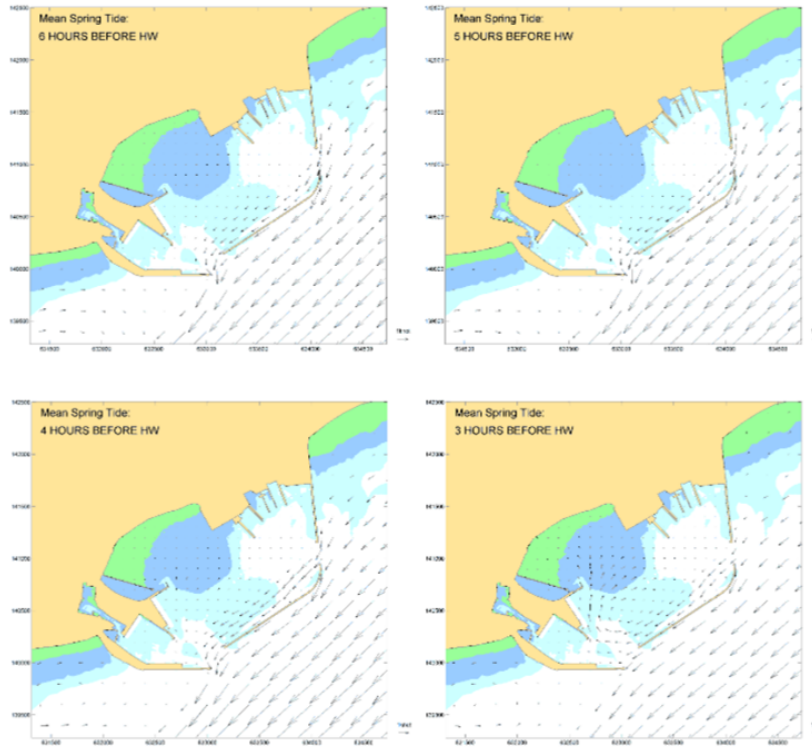


Figure 7: A selection of the mean tidal flows observed at 6, 5, 4 and 3 hours before high water. Produced by The Port of Dover Institution (Masters 2019)

high water will affect the harbour. Using this data as a visual comparison the data collected using the lid-driven method has been able to capture some of the distinct features within the tidal system.

When leading up to the high water tidal effect the current rides over the top of the harbour creating this lid-driven effect. Due to the east flowing tides this feature can be simplified as a driven lid. Then during the high tide phenomena a distinct vortex is created within the harbour as can be seen in Figures 5c, 5d, 6c and 6d. Despite this the figures do not represent as clear of a vortex shown in the report.

The breakwater featured at Dover Harbour seems to be adequate and not needed to be adapted. According to the simulations and the tidal data provided in (Vernon-Harcourt 1885), it provides adequate protection from both the English Channel and the North Sea tidal currents that flow past the harbour, as well as being large enough to accommodate larger ferry vessels.

The most extreme velocity speeds are found within the back of the harbour as seen in Figures 6c and 6d nearer the boundaries. This could affect vessels, particularly the smaller boats as a strong current can be seen flowing in from the northeastern-most entrance and leading into the area that would house them. The larger vessels, situated upon the southwestern-most entrance experiences the greatest change in velocity.

5 Conclusions

The LBM has been able to utilise the lid-driven cavity problem with respect to harbours. The lid-driven cavity problem has provided a useful look into the effect the tidal currents have upon the inner flows of Dover Harbour. Although it is an idealised case it was able to show some of the features necessary for the high water flows. For further study areas the tidal height and sub-level geographical features will be taken into account.

When observing the mean tidal data a good comparison can be drawn between the two models, however further testing must be undertaken. To get a better observation water height should be added into the cavity model and observing the ebbs and flood tides at different times.

6 Acknowledgement

I would like to acknowledge and thank both my supervisors, Dr Jian Zhou and Jon Shiach for providing me with this opportunity.

References

- Bhatnagar, P. L., E.P. Gross, and M. Krook (1953). *A Kinetic Approach to Collision Processes in Gases: Small Amplitude Processes in Charged and Neutral One Component Systems*. Tech. rep. Massachusetts: Massachusetts Institute of Technology.
- Bowden, K. F. (Feb. 1956). “The Flow of Water through the Straits of Dover, Related to Wind and Differences in Sea Level”. In: *Philosophical Transactions of the Royal Society A: Mathematical, Physical and Engineering Sciences* 248.953, pp. 517–551. ISSN: 1364-503X. doi: 10.1098/rsta.1956.0008.
- Ghia, U, K N Ghia, and C T Shin (1982a). *High-Re Solutions for Incompressible Flow Using the Navier-Stokes Equations and a Multigrid Method**. Tech. rep., pp. 387–411.
- (1982b). *High-Resolutions for Incompressible Flow Using the Navier-Stokes Equations and a Multigrid Method**. Tech. rep., pp. 387–411. URL: <http://citeseerx.ist.psu.edu/viewdoc/download;jsessionid=72463FA5559BD27ED04B329C92DDBCC8?doi=10.1.1.413.9651&rep=rep1&type=pdf>.
- Guo, Zhaoli, Baochang Shi, and Nengchao Wang (2000). “Lattice BGK Model for Incompressible Navier-Stokes Equation”. In: *Article in Journal of Computational Physics* 165, pp. 288–306. doi: 10.1006/jcph.2000.6616. URL: https://www.researchgate.net/profile/Zhaoli_Guo2/publication/222537628_Lattice_BGK_Model_for_Incompressible_Navier-Stokes-Equation/links/59ed5a2e4585151983ccdd66/Lattice-BGK-Model-for-Incompressible-Navier-Stokes-Equation.pdf.
- Huang, Changsheng et al. (2015). “Multi-GPU based lattice boltzmann method for hemodynamic simulation in patient-specific cerebral aneurysm”. In: *Communications in Computational Physics*. ISSN: 19917120. doi: 10.4208/cicp.2014.m342.

- Latteux, B. (1980). “Harbour Design Including Sedimentological Problems Using Mainly Numerical Techniques”. In: *Coastal Engineering*.
- Masters, Steve. (2019). *Mean Spring Tide Tidal Currents*. Tech. rep. Dover: Port of Dover, p. 5.
- McNamara, Guy R. and Gianluigi Zanetti (Nov. 1988). “Use of the Boltzmann Equation to Simulate Lattice-Gas Automata”. In: *Physical Review Letters* 61.20, pp. 2332–2335. ISSN: 0031-9007. DOI: 10.1103/PhysRevLett.61.2332. URL: <https://link.aps.org/doi/10.1103/PhysRevLett.61.2332>.
- Mohammed, Seemaa and Tim Reis (2017). “Using the Lid-Driven Cavity Flow to Validate Moment-Based Boundary Conditions for the Lattice Boltzmann Equation”. In: *Mechanical Engineering* 64.1, pp. 59–74. DOI: 10.1515/meceng-2017-0004. URL: <https://www.degruyter.com/downloadpdf/j/meceng.2017.64.issue-1/meceng-2017-0004/meceng-2017-0004.pdf>.
- Nie, Xiaobo and Nicos S. Martys (2007). “Breakdown of Chapman-Enskog expansion and the anisotropic effect for lattice-Boltzmann models of porous flow”. In: *Physics of Fluids*. ISSN: 10706631. DOI: 10.1063/1.2432153.
- Perumal, D. Arumuga and Anoop K. Dass (Mar. 2013). “Application of lattice Boltzmann method for incompressible viscous flows”. In: *Applied Mathematical Modelling* 37.6, pp. 4075–4092. ISSN: 0307-904X. DOI: 10.1016/J.APM.2012.09.028. URL: <https://www.sciencedirect.com/science/article/pii/S0307904X12005252>.
- Prandle, D. et al. (June 1993). “The influence of horizontal circulation on the supply and distribution of tracers”. In: *Philosophical Transactions of the Royal Society of London. Series A: Physical and Engineering Sciences* 343.1669, pp. 405–421. DOI: 10.1098/rsta.1993.0055. URL: <http://www.royalsocietypublishing.org/doi/10.1098/rsta.1993.0055>.
- Sanchez-Arcilla, A. et al. (2002). “Water Renovation in Harbour Domains. The Role of Wave and Wind Conditions”. In: *Coastal Engineering 2002*. WORLD SCIENTIFIC. ISBN: 978-981-238-238-2.
- Vernon-Harcourt, L.F. (1885). *Harbours and Docks*. Cambridge: Cambridge University Press, p. 650. ISBN: 978-1-108-07202-1. URL: <https://books.google.co.uk/books?hl=en&lr=&id=4Wk3BAAQBAJ&oi=fnd&pg=PR3&dq=tidal+currents++Dover+harbours&ots=nahxrVzW1Q&sig=720Wz7Q-XThebZ06tYsxqXbFFBo#v=onepage&q=Dover&f=false>.
- Wolf-Gladrow, Dieter A. (2000). *Lattice Gas Cellular Automata and Lattice Boltzmann Models*. ISBN: 978-3-540-66973-9. DOI: 10.1007/b72010.
- Zou, Qisu and Xiaoyi He (1997). “On pressure and velocity flow boundary conditions and bounce-back for the lattice Boltzmann BGK model”. In: *Physics of Fluids* 9.6, pp. 1591–1598. DOI: 10.1063/1.869307.